Available online at www.sciencedirect.com
SCIENCE DIRECT®
Journal of Photochemistry and Photobiology A: Chemistry 167 (2004) 141–148
Journal of Photochemistry and Photobiology A:Chemistry
www.elsevier.com/locate/jphotochem

Characterizing pyrene–Ag^+ exciplex formation in aqueous and ethanolic solutions

Ji Hoon Lee [a,b], Elizabeth R. Carraway [a,b,*], Mark A. Schlautman [a,b,1], Soobin Yim [b], Bruce E. Herbert [c]

[a] *School of the Environment, Clemson University, Clemson, SC 29634-0919, USA*
[b] *Clemson Institute of Environmental Toxicology, Clemson University, Pendleton, SC 29670, USA*
[c] *Department of Geology and Geophysics, Texas A&M University, College Station, TX 77843, USA*

Received 30 July 2003; received in revised form 12 April 2004; accepted 22 April 2004
Available online 24 June 2004

Abstract

The primary mechanism responsible for the dynamic fluorescence quenching of polycyclic aromatic compounds (PACs) by Ag^+ ions is enhanced intersystem crossing from the lowest singlet excited state to the lowest triplet excited state. For some PACs, however, exciplex formation with Ag^+ in polar organic solvents has also been reported. Quenching of pyrene fluorescence by Ag^+ in two polar solvent systems (aqueous and ethanolic solutions) was examined here using steady-state and time-resolved fluorescence techniques. In both solvents, quenching led to the formation of a pyrene–Ag^+ exciplex, $(^1Py\cdots Ag^+)^*$, which rapidly equilibrated with excited singlet pyrene molecules ($^1Py^*$) and Ag^+ ions. The exciplex and pyrene monomer emission spectra strongly overlapped, with the dominant exciplex peaks in water and ethanol red shifted from the 0–0 transition of pyrene by 5.08 and 2.56 kJ/mol, respectively. Rate constants for the formation and dissociation of the exciplex were much larger than the radiative and nonradiative decay rate constants for both the excited state monomer and exciplex. The short exciplex fluorescence lifetimes and very low quantum yields observed in the two solvents can be attributed to enhanced nonradiative decay processes for the exciplex. The emission quantum yield of the exciplex formed in aqueous solution was approximately an order of magnitude larger than that in ethanolic solution, which is likely to be attributable to the higher polarity of water versus ethanol.

Keywords: Time-resolved fluorescence; Steady-state fluorescence; Dynamic quenching; Fluorescence lifetime; Rate constants; Quantum yield; Silver ion

1. Introduction

It has been known for some time that mixed or heteroexcimers (i.e., exciplexes), formed from the interaction between a singlet excited state fluorophore and a quencher, can be intermediates in some fluorescence quenching processes [1,2]. The stability of exciplexes is generally restricted to nonpolar solvents, because in polar solvents the transient complex typically dissociates into radical ions due to the stabilization energy available via solvation [3]. However, even though exciplex formation is observed predominantly in solvents having relatively small dielectric constants, several research groups have recently reported properties of exciplexes formed in polar organic solvents [4–7]. For example, Dreeskamp and coworkers [8,9] demonstrated the formation of an exciplex between perylene and Ag^+ ions in polar organic solvents and proposed the reaction model shown in Scheme 1. In this scheme, k_1 and k_2 are overall rate constants for excited monomer and exciplex relaxation, respectively, and k_a and k_d are rate constants for the formation and dissociation of the exciplex, respectively. Dreeskamp and coworkers also investigated exciplex formation between other polycyclic aromatic compounds (PACs) and Ag^+ in polar organic solvents based on Scheme 1 [10]. For all PACs studied, Dreeskamp and coworkers showed that k_a is much larger than k_d.

The results of Dreeskamp and coworkers [8–10] suggest that some portion of PAC fluorescence quenching by Ag^+ ions in polar solvents may be due to exciplex formation. Other research groups [11–13], however, did not observe exciplex emission from pyrene and various metal ions, and instead proposed intersystem crossing (ISC) as the mechanism responsible for fluorescence quenching. For

* Corresponding author. Tel.: +1-864-646-2189; fax: +1-864-646-2277.
E-mail addresses: ecarraw@clemson.edu (E.R. Carraway), mschlau@clemson.edu (M.A. Schlautman).
[1] Co-corresponding author. Tel.: +1-864-656-4059; fax: +1-864-656-0672.

1010-6030/$ – see front matter © 2004 Elsevier B.V. All rights reserved.
doi:10.1016/j.jphotochem.2004.04.012

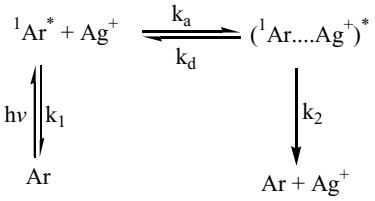

Scheme 1.

example, based on transient absorption spectra, Saito et al. [11] proposed that the quenching of pyrene fluorescence by Ag^+ in ethanol was due to triplet state formation from $^1Py^*$. Nosaka et al. [12] proposed that the quenching of fluorescence from pyrene–caffeine complexes by Ag^+ ions in caffeine-solubilized aqueous solution was due to accelerated ISC of $^1Py^*$ and enhanced internal conversion, both brought about by the electron distortion resulting from caffeine-pyrene–Ag^+ complexes in the ground state. Based on results of pyrene fluorescence quenching by metal ions in sodium dodecyl sulfate micelle solutions, Nakamura et al. [13] reported that complexes such as $(^1Py\cdots Ag^+)^*$, which are formed diffusionally with an efficiency depending upon the specific metal ion, enhance the mixing of spin states leading to ISC. Nakamura et al. also suggested that enhanced ISC resulting from complex formation in the excited state might be applicable to conventional organic solvents as well as aqueous micellar solutions.

Recently, we reported on a novel technique that uses fluorescence quenching to quantify ground-state complexes between PACs and Ag^+ in dilute aqueous solution [14]. For molecules such as naphthalene, Ag^+ complexation constants can be determined directly from their steady-state and time-resolved fluorescence data. However, for pyrene we found that additional steps were necessary to obtain its Ag^+ complexation constants. These additional steps were needed to correct for a wavelength-dependent emission interference, presumably resulting from a pyrene–Ag^+ exciplex [14]. In this study, we examine in more detail the quenching of pyrene fluorescence by Ag^+ ions in aqueous and ethanolic solutions to determine if similar photophysical processes occur in these two polar solvent systems and to identify whether exciplex formation may be a contributing component to the dynamic quenching of pyrene fluorescence in these solvents.

2. Experimental

2.1. Chemicals

$AgClO_4$ (99.9%), $NaClO_4$ (99.0%), naphthalene (99.0%), pyrene (99.0%) and HPLC-grade ethanol (denatured with 5% isopropanol and 5% methanol) were purchased from Aldrich and used without further purification. Spectroscopic grade methanol and glycerol (99.6%, Certified A.C.S.) were purchased from Fisher Scientific. Distilled, deionized water (Super-Q^{TM} Plus, Millipore) having a resistivity greater than 18.0 MΩ cm was used to prepare all aqueous solutions.

2.2. General procedures

Pyrene, naphthalene and $AgClO_4$ stock solutions were prepared at room temperature (21 ± 2 °C) and stored in dark containers to minimize photoreactions. Samples for fluorescence measurements were prepared in an anaerobic chamber (95% N_2, 5% H_2; Coy Laboratory Products Inc.) using deoxygenated solvents and then sealed in 1 cm screw cap anaerobic fluorescence cells (Starna) to exclude oxygen. The ionic strength of most samples was fixed at 0.1 M with $NaClO_4$, except for selected studies that used higher Ag^+ concentrations (0.1 to 0.2 M) to confirm/refute its formation of an exciplex with pyrene and naphthalene. In general, Na^+ and ClO_4^- are not considered to be quenchers of PAC fluorescence [15]. Also, $AgClO_4$ and $NaClO_4$ solutions have no appreciable absorption bands at wavelengths longer than 300 nm [16].

Ultraviolet–visible (UV–vis) absorption spectra (resolution of 0.05 nm) were measured with a double-beam, double-monochromator spectrophotometer (Shimadzu 2501PC) using appropriate background solutions as references. Steady-state fluorescence spectra were recorded with a PTI QuantaMaster^{TM} spectrometer (Photon Technology International, Inc.) equipped with a 75 W xenon arc lamp. The primary excitation wavelength used for pyrene was 334 nm, and fluorescence emission was monitored over a wavelength range of 370 to 455 nm. When necessary, observed fluorescence intensities were corrected for inner filter effects and/or Raman scattering from the background solution [17,18]. For a limited number of experiments, an excitation wavelength of 304 nm was used to confirm the results obtained with 334 nm. For example, pyrene fluorescence spectra in the absence and presence of Ag^+ ions had to be corrected for Raman scattering when the excitation wavelength was 334 nm. To ensure that this correction did not create artifacts in the spectra, the corrected spectra were compared to those obtained using an excitation wavelength of 304 nm for which Raman scattering did not interfere with pyrene emission. In all cases, corrected spectra for 334 nm were identical to those obtained using 304 nm. Excitation and emission slits were adjusted to a resolution of 0.25 nm. Steady-state fluorescence spectra emission areas were determined using the integrating tool in Origin 6.0 (Microcal Software, Inc.). Fluorescence lifetimes and time-resolved fluorescence spectra were obtained with a PTI TimeMaster^{TM} spectrometer using a nitrogen-filled nanosecond flashlamp and a stroboscopic optical boxcar detection methodology. Pyrene monomer and exciplex emission decay lifetimes were determined at wavelengths corresponding to the major bands of pyrene's vibrational fine structure (e.g., $I_1 = 373$ nm, $I_2 = 379$ nm, $I_3 = 383$ nm, $I_4 = 389$ nm, $I_5 = 393$ nm). Lifetime data analyses were performed using TimeMaster Pro^{TM} for Windows provided

with the PTI system. Observed fluorescence decays were deconvoluted using a sum of exponentials model and a measured excitation pulse by the Marquardt nonlinear least-squares method. Goodness of fit was characterized by the reduced chi-square statistic (χ^2), Durbin–Watson parameter, runs test, and plots of the weighted residuals and the autocorrelation function of weighted residuals. Best fit values for the pre-exponential factors (A_i) and lifetimes (τ_i) were then utilized in subsequent calculations and analyses.

3. Results and discussion

3.1. Evidence for pyrene–Ag^+ exciplex formation in aqueous and ethanolic solutions

Representative steady-state pyrene fluorescence emission spectra in the absence and presence of Ag^+ ions (0.12 M) are shown in Fig. 1a and b for aqueous and ethanolic solutions, respectively. Because Ag^+ strongly quenched the pyrene fluorescence, the corresponding curves were normalized to a value of 1 at the 0–0 transition (373 nm), where the least amount of emission interference occurred [14]. Differences between spectra such as those shown in Fig. 1a and b have previously been attributed to exciplex emission [8–10], presumably resulting here from a $(^1Py\cdots Ag^+)^*$ exciplex. To confirm that the normalization procedure did not create artifacts due to a poor signal-to-noise response in lieu of highlighting the presence of an exciplex, we performed the same normalization procedure (75×) on the spectrum of a diluted (4.5×10^{-9} M) pyrene solution with no Ag^+ and observed that the corresponding curves were identical when normalized to a value of 1 at the 0–0 transition (373 nm) (data not shown).

As noted in the Introduction, exciplex formation is observed predominantly in relatively nonpolar solvent systems. For the spectra shown in Fig. 1, then, several considerations might suggest against the possibility of exciplex formation. First, the emission from the proposed exciplex is relatively close in energy to that of pyrene itself, which might have

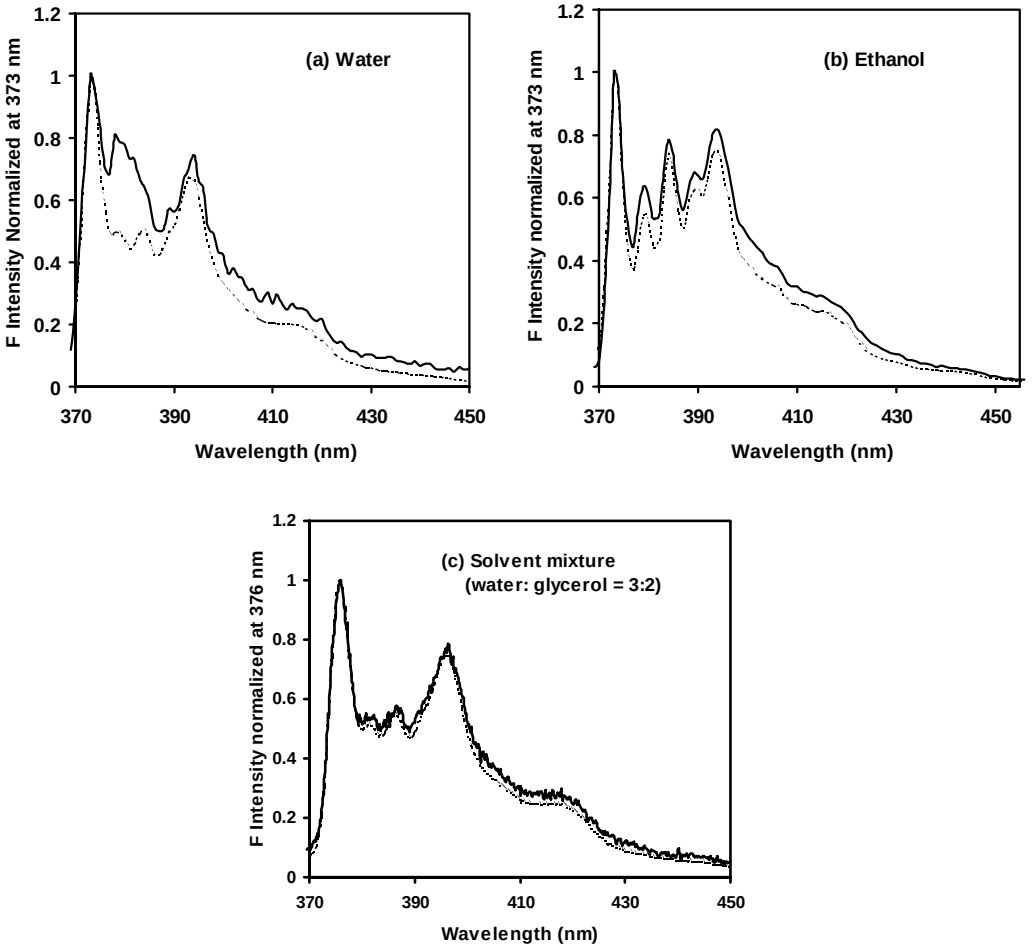

Fig. 1. Representative steady-state fluorescence emission spectra of pyrene in the absence (– – –) and presence (—) of 0.12 M $AgClO_4$. The curves were normalized to a value of one at the 0–0 transition to highlight the presence of the exciplex. (a) Aqueous solution. Measurement conditions: [Pyr] = 4.5×10^{-7} M, λ_{ex} = 334 nm, λ_{0-0} = 373 nm. (b) Ethanolic solution. Measurement conditions: [Pyr] = 2.0×10^{-5} M, λ_{ex} = 334 nm, λ_{0-0} = 373 nm. (c) 60–40% water–glycerol mixture. Measurement conditions: [Pyr] = 4.5×10^{-7} M, λ_{ex} = 336 nm, λ_{0-0} = 376 nm.

been expected to lead to formation of radical ion products [3] or the pyrene triplet state due to enhanced ISC via spin orbit coupling in the presence of Ag^+ [11–13]. Regarding the latter scenario, however, it is important to note that the primary fluorescence quenching mechanism for pyrene in these two solvents was likely ISC, consistent with the large normalization factors needed to highlight the exciplex emission in Fig. 1 and with the very small estimated exciplex quantum yields (see below). Second, since it is known that pyrene forms ground-state complexes with Ag^+, one might argue that the observed emission resulted from ground-state complexes rather than from a pyrene–Ag^+ exciplex. However, additional measurements made to test this ground-state complex hypothesis appeared to rule out this possibility. For example, steady-state fluorescence excitation scans in the absence and presence of high concentrations of Ag^+ in water and ethanol did not reveal the presence of emissive ground-state complexes (data not shown). In addition, steady-state fluorescence emission scans of pyrene and Ag^+ in 60–40% (by mass) water–glycerol mixtures were indistinguishable from those measured in the absence of Ag^+ (Fig. 1c). Because this, latter solvent mixture has a dielectric constant between that of pure water and ethanol but a viscosity of ∼3.7 cP, the result clearly demonstrates that the emission in question results from a diffusional process (i.e., exciplex formation) rather than from a ground-state complex. Finally, to further verify our results, we performed the same types of experiments and analyses as those described above using naphthalene, but never detected any evidence of emission resulting from a naphthalene–Ag^+ exciplex. These observations with naphthalene also provide additional support for the idea that PAC–Ag^+ ground-state complexes are not emissive.

To better delineate the exciplex emission versus that of the pyrene monomer, all fluorescence emission spectra were ratioed to the unquenched spectrum and then normalized to a value of one at the 0–0 transition band (Fig. 2a and b). In aqueous solution, a broad, relatively featureless exciplex emission band can be observed in the wavelength region 375–385 nm (Fig. 2a). This band, centered at approximately 379 nm and coincident with the second vibrational peak (I_2) of the pyrene fine structure [19], is shifted to the red (5.08 kJ/mol) as compared to the 0–0 transition (373 nm) of pyrene. In ethanolic solutions, however, exciplex emission spectra appear to have four maxima between 370 and 395 nm (Fig. 2b). These peaks, centered at approximately 376, 380, 386 and 391 nm, respectively, generally fall between the peaks associated with the pyrene monomer emission fine structure. The strongest band at 376 nm is red-shifted approximately 2.56 kJ/mol, as compared to the 0–0 transition of pyrene.

Pyrene monomer fluorescence has five predominant peaks resulting from different vibrational levels, some of which are sensitive to the molecular solvent environment. For example, Kalyanasundaram and Thomas [19] have shown that the I_1/I_3 ratio (or, alternatively, the reciprocal I_3/I_1 ratio) of pyrene is correlated with solvent polarity as measured by the dielectric constant. Our attempts to use steady-state measurements of the I_1/I_3 ratio to monitor potential changes in pyrene solvation in water upon addition of $AgClO_4$ were generally unsuccessful due to the overlapping exciplex emission. Time-resolved emission spectra acquired after appropriate detection delay times (e.g., 30 ns) removed the exciplex interference (data not shown), but instrument sensitivity limited this approach to solutions of relatively low Ag^+ concentration (<5 mM). These low concentrations, in turn, did not allow for adequate resolution of a significant I_1/I_3 trend with [Ag^+].

Because the maximum exciplex emission band in aqueous solution was observed near the second vibrational peak, we used the I_2/I_1 ratio in the present study to follow formation of the exciplex (Fig. 2c). Although none of the exciplex emission peaks coincided with 379 nm in ethanolic solutions, the I_2/I_1 ratio could be used to monitor exciplex formation in that solvent as well. This was verified by the identical slopes of the regression lines for the ratio using I_2 and ratios using the exciplex emission maxima wavelengths of 376 and 380 nm. In both aqueous and ethanolic solutions, the I_2/I_1 ratio increases linearly with increasing Ag^+ concentration indicating that the height of I_2 and thus the exciplex concentration is directly dependent on the Ag^+ ion concentration, consistent with Scheme 1.

As previously noted, formation of an exciplex generally occurs only in nonpolar solvents because of its tendency to dissociate to radical ions in polar solvents ($\varepsilon > 20.0$) [20]. Recently, however, several research groups have reported exciplex formation in polar organic solvents such as acetone, methanol and acetonitrile ($\varepsilon = 20.7$, 32.6 and 37.5, respectively) [4–10]. Figs. 1 and 2 demonstrate that $(^1Py \cdots Ag^+)^*$ exciplex formation is also possible in aqueous solution, which has a very high dielectric constant ($\varepsilon = 80.1$).

Time-resolved fluorescence measurements were made to verify formation of the exciplex in aqueous and ethanolic solutions and test the above assumptions related to the steady-state emission spectra. Fig. 3 shows a representative fluorescence-decay curve at I_2 for pyrene in aqueous solution with 5.0 mM $AgClO_4$. Values in Table 1 show that fluorescence lifetimes of the pyrene monomer (τ) in aqueous solution systematically decrease with increasing $AgClO_4$ concentration, but that the fluorescence lifetime of the exciplex (τ_{exc}) is relatively constant and independent of $AgClO_4$ concentration. In addition, the pyrene monomer fluorescence lifetimes measured at I_2 (Table 1) are consistent with those determined at I_1 and the other selected wavelengths within the limits of uncertainty [14]. Results in Table 1 provide confirmatory evidence to Figs. 1 and 2 for the formation of an exciplex in aqueous solution. Similar trends with Ag^+ ion concentration were observed for τ and τ_{exc} in ethanolic solutions (data not shown), again confirming the formation of an exciplex in that solvent system. Finally, it is noteworthy that the values of τ_{exc} measured in our two solvent systems

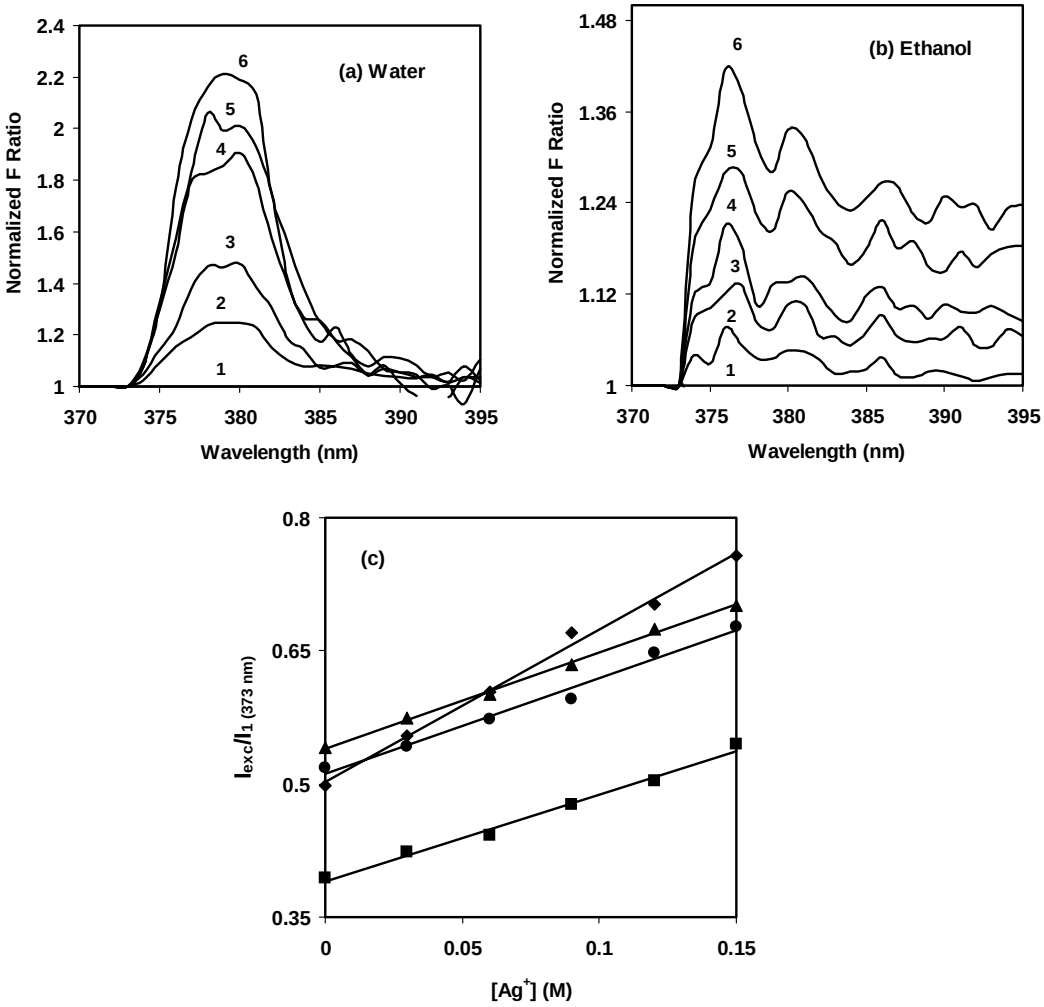

Fig. 2. Representative normalized steady-state fluorescence spectra ratios for aqueous (a) and ethanolic (b) solutions with Ag^+ concentrations of 0 (1), 0.03 (2), 0.06 (3), 0.09 (4), 0.12 (5), and 0.15 M (6). The effect of Ag^+ concentration on exciplex formation as monitored by changes in apparent fine structure ratios is shown in (c) for aqueous pyrene (4.5×10^{-7} M; (◆) I_{379}/I_{373}) and ethanolic pyrene (2.0×10^{-5} M; (■) I_{376}/I_{373}, (▲) I_{379}/I_{373}, (●) I_{380}/I_{373}) solutions.

Table 1
Fluorescence decay parameters at I_2 (379 nm) for aqueous pyrene solutions (4.5×10^{-7} M) upon addition of $AgClO_4$[a]

[$AgClO_4$] (mM)	τ (ns)	τ_{exc} (ns)	A[b], 10^{-3}	A_{exc}[b], 10^{-3}	χ^2[c]	τ_{eff}[d] (ns)	A_{eff}[b], 10^{-3}	χ^2[c]
0	210.0 (4.1)	–	7.5 (0.10)	–	1.03	210.0 (4.1)	7.5 (0.10)	1.03
1.0	135.7 (2.3)	3.6 (0.3)	6.9 (0.06)	5.3 (0.07)	1.04	113.2 (3.1)	7.4 (0.10)	1.45
2.0	88.5 (1.9)	3.8 (0.3)	6.7 (0.09)	5.1 (0.04)	0.94	79.6 (2.1)	7.6 (0.06)	1.62
3.0	70.1 (1.4)	3.7 (0.4)	6.4 (0.05)	4.9 (0.07)	0.91	62.3 (1.3)	7.3 (0.10)	1.08
4.0	57.6 (2.6)	3.2 (0.3)	6.2 (0.08)	5.3 (0.05)	0.87	48.4 (2.0)	7.3 (0.06)	1.24
5.0	44.9 (1.5)	3.4 (0.2)	6.1 (0.05)	5.2 (0.07)	0.75	39.3 (1.2)	7.1 (0.09)	1.08

[a] Mean values and standard errors (in parentheses) were obtained from double or single exponential model fits to the fluorescence lifetime data.
[b] Relative amplitudes of each component.
[c] Reduced chi-square statistic for each best fit. For all double exponential fits, the Durbin–Watson parameter was always greater than 1.75 and the Runs Test always generated values of $Z > -1.96$, indicating satisfactory fits at the 95% confidence level.
[d] Single exponential fluorescence lifetime consistent with the assumptions that $k_3[Q]$ and k_4 are much larger than $(k_1 + k_2)$ and k_p (see Scheme 2).

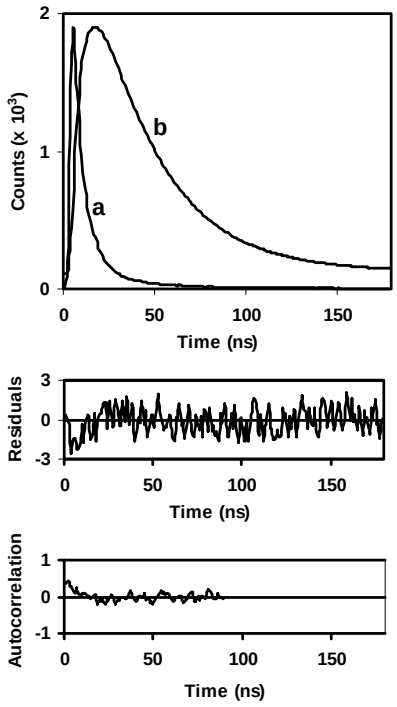

Fig. 3. Representative fluorescence decay curve of pyrene (4.5×10^{-7} M) in aqueous solution in the presence of 5.0×10^{-3} M $AgClO_4$ measured at 379 nm (curve b) plotted together with the lamp–pulse profile (curve a). The decay curve was best fit by deconvolution using a double exponential model with $\tau = 44.9 \pm 1.5$ ns and $\tau_{exc} = 3.4 \pm 0.2$ ns (Table 1).

are much longer than the reported lifetimes of radical ion pairs [21,22].

3.2. Rate constants for pyrene–Ag+ exciplex processes

A detailed kinetic scheme for $(^1Py \ldots Ag^+)^*$ exciplex formation and decay in aqueous and ethanolic solutions adapted from previous reports [2,7,23] is shown in Scheme 2, where k_1 and k_2 are the radiative and nonradiative decay rate constants of excited state pyrene monomer, k_3 and k_4 are the formation and dissociation rate constants of the exciplex, and k_5 and k_6 are the radiative and nonradiative decay rate constants of the exciplex. In Scheme 2, the nonradiative decay pathways (2 and 6) are likely due to a combination of mechanisms such as ISC and internal

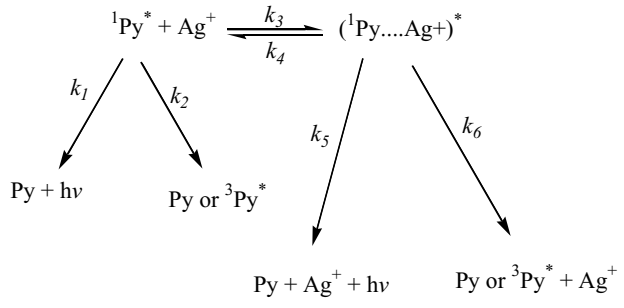

Scheme 2.

conversion. An equation to quantify the dynamic quenching of pyrene monomer fluorescence can be derived from the Stern–Volmer equation and Scheme 2 [2,7,23]:

$$\frac{\tau_0}{\tau} = k_q \tau_0 [Q] + 1 = \frac{k_3 k_p \tau_0 [Q]}{k_4 + k_p} + 1 \quad (1)$$

where τ_0 and τ are the pyrene monomer fluorescence lifetimes in the absence and presence of Ag^+ ions, respectively, $[Q]$ is the concentration of the quencher (Ag^+ ions), and

$$k_p = (k_5 + k_6) = \frac{1}{\tau_{exc}} \quad (2)$$

The bimolecular quenching constant, k_q, for the present system can therefore be expressed as:

$$k_q = \frac{k_3 k_p}{k_4 + k_p} \quad (3)$$

In aqueous solution, the k_q value of $(3.31 \pm 0.09) \times 10^9\ M^{-1}\ s^{-1}$, calculated using Eq. (1) and the monomer τ values from Table 1, is larger than the k_p value of $(2.79 \pm 0.18) \times 10^8\ s^{-1}$, calculated from the τ_{exc} values also from Table 1. Similarly, the k_q value of $(1.72 \pm 0.07) \times 10^9\ M^{-1}\ s^{-1}$ determined in ethanol is larger than the k_p value of $(3.09 \pm 0.12) \times 10^8\ s^{-1}$.

Previous researchers [2,7,23] have demonstrated that if $k_3[Q]$ and k_4 are much larger than $(k_1 + k_2)$ and k_p, then equilibrium between $^1Py^*$ and $(^1Py \cdots Ag^+)^*$ will be reached very quickly in Scheme 2. In this situation, an effective decay rate constant (k_{eff}) for both species combined will be close to a single-exponential decay rate ($1/\tau_{eff}$) as expressed in Eq. (4) [2,7,23]:

$$k_{eff} = \tau_{eff}^{-1} = (k_1 + k_2)\left(\frac{k_4}{k_4 + k_3[Q]}\right) + k_p\left(\frac{k_3[Q]}{k_4 + k_3[Q]}\right) \quad (4)$$

From Eq. (4), the effective pyrene fluorescence lifetime (τ_{eff}) in the presence of Ag^+ ions is:

$$\tau_{eff} = \frac{1 + K[Q]}{\tau_0^{-1} + K k_p [Q]} \quad (5)$$

where $K = (k_3/k_4)$ is the equilibrium constant for exciplex formation. Rearranging Eq. (5), the Stern–Volmer equation for dynamic quenching can then be expressed as:

$$\frac{\tau_0}{\tau_{eff}} = \frac{1 + K k_p \tau_0 [Q]}{1 + K[Q]} \quad (6)$$

To obtain K and k_p from the pyrene dynamic quenching data in Table 1, Eq. (6) can be rearranged to a linear form for simplicity:

$$(\tau_{eff}^{-1} - \tau_0^{-1})^{-1} = K^{-1}(k_p - \tau_0{}^{-1})^{-1}[Q]^{-1} + (k_p - \tau_0{}^{-1})^{-1} \quad (7)$$

Fig. 4 shows representative plots of $(\tau_{eff}^{-1}\tau_0^{-1})^{-1}$ versus $[Q]^{-1}$ generated from our values obtained in aqueous and

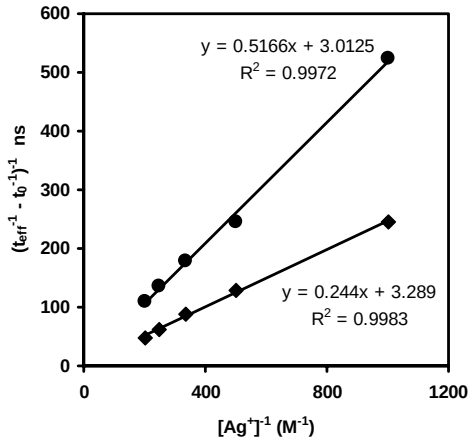

Fig. 4. Plots of Eq. (7) for representative data sets to determine the exciplex equilibrium constant, $K = k_3/k_4$, and observed rate constant for direct loss of energy from the exciplex, k_p, based on the assumptions that $k_3[Q]$ and k_4 are much larger than $(k_1 + k_2)$ and k_p in Scheme 2. (◆) aqueous solution, (●) ethanol.

ethanolic solutions. From the slope and intercept of each regression line, values for k_p and K can then be calculated. The k_p values determined with this technique were consistent with (i.e., within 10% of) the values previously calculated from the experimental τ_{exc} values in aqueous and ethanolic solutions. The excellent regressions obtained (Fig. 4) and consistent k_p values indicate that the assumptions leading to Eqs. (4)–(7) are valid in the present systems.

Despite very different solvent polarities ($\varepsilon = 80.1$ and 24.3 for water and ethanol, respectively), k_p values in aqueous and ethanolic solutions were similar (i.e., within 5%) and consistent with trends reported by Rath et al. [7]. Conversely, the value for K in aqueous solution was more than a factor of two larger than its corresponding value in ethanolic solution, indicating that the exciplex is more stable in water than ethanol. With the values above for K and k_p, the previously determined values for k_q, and using Eq. (3), values for k_3 and k_4 were also computed. Finally, a value for $(k_1 + k_2)$ was calculated with Eq. (4) using all previously determined rate constants (Table 2).

3.3. Quantum yield considerations

Monomer and exciplex quantum yields pertinent to Scheme 2 have been defined by Ware et al. [2]:

$$\Phi^0_{mo} \equiv \frac{k_1}{k_1 + k_2} \tag{8}$$

$$\Phi_{exc} \equiv \frac{k_5}{k_4 + k_p} \tag{9}$$

where Φ^0_{mo} is the quantum yield of the monomer in the absence of quencher and Φ_{exc} is the quantum yield of the exciplex. If the monomer and exciplex fluorescence intensities (I_{mo} and I_{exc}) measured in the presence of quencher are integrated over their entire emission bands, then the ratio

Table 2
Kinetic and equilibrium parameters for Scheme 2[a]

	Aqueous solution	Ethanolic solution
k_q ($M^{-1}\,s^{-1}$)	3.31 (0.09) × 10^9	1.72 (0.07) × 10^9
$k_1 + k_2$ (s^{-1})[b]	4.76 (0.08) × 10^6	3.68 (0.03) × 10^6
k_1 (s^{-1})[c]	3.28 (0.05) × 10^6	2.39 (0.02) × 10^6
k_2 (s^{-1})[c]	1.48 (0.03) × 10^6	1.29 (0.01) × 10^6
k_3 ($M^{-1}\,s^{-1}$)[d]	1.62 (0.03) × 10^{10}	2.50 (0.05) × 10^{10}
k_4 (s^{-1})[d]	1.18 (0.02) × 10^9	4.29 (0.06) × 10^9
k_p (s^{-1})[e]	3.04 (0.01) × 10^8	3.16 (0.01) × 10^8
k_5 (s^{-1})[f]	7.85 (0.03) × 10^5	2.43 (0.02) × 10^5
k_6 (s^{-1})[g]	3.03 (0.01) × 10^8	3.16 (0.01) × 10^8
K (M^{-1})[e]	13.7 (0.2)	5.8 (0.2)
Φ_{exc}	5.30 (0.10) × 10^{-4}	5.27 (0.06) × 10^{-5}

[a] Mean values and standard errors (in parentheses) were determined from three independent replicate experiments.
[b] From Eq. (4).
[c] Unique values for k_1 and k_2 determined from their sum and Eq. (8) using representative values of Φ^0_{mo} for the two solutions.
[d] From Eq. (3).
[e] From Eq. (7) and Fig. 4. Values for k_p were within 10% of those determined from the average τ_{exc} (Table 1).
[f] From Eq. (10).
[g] From Eq. (2).

of integrated intensities can be used to estimate the ratio of the two quantum yields (Φ_{exc}/Φ_{mo}) [2]. For this case, k_5 then can be computed using the following equation [2]:

$$k_5 = \frac{k_1(k_4 + k_p)\Phi_{exc}}{k_3\Phi_{mo}[Q]} \tag{10}$$

To use Eq. (10), representative values of Φ^0_{mo} were first selected for pyrene in each solution (0.69 and 0.65 for aqueous [24,25] and ethanolic [26] solutions, respectively), and then k_1 values were obtained using Eq. (8) and the values for $(k_1 + k_2)$ determined above. As shown in Figs. 1 and 2, it was not possible to compute an exact exciplex quantum yield (Φ_{exc}) in the present systems because of the extensive overlap of the pyrene monomer and exciplex emission bands. However, we were able to estimate the Φ_{exc}/Φ_{mo} ratio by integrating the areas under the monomer spectra and their corresponding exciplex spectra, which were assumed to be the difference spectra obtained from normalized curves such as those shown in Fig. 1. We then computed k_5 using Eq. (10) with all the previously determined parameter values. All rate and equilibrium constants that we were able to obtain for the processes in Scheme 2 are listed in Table 2.

Using Eq. (9) and the appropriate kinetic values from Table 2, we were able to calculate approximate values of Φ_{exc} for $(^1Py\cdots Ag^+)^*$ in both solutions. The Φ_{exc} value in water (5.30×10^{-4}), computed in this manner, was approximately an order of magnitude larger than that in ethanol (5.27×10^{-5}). Although this difference was much larger than the relative difference in Φ^0_{mo} values for the two solutions, it appears to be consistent with reports that the relative efficiency of ISC from the singlet exciplex, $(^1Py\cdots Ag^+)^*$, to the triplet state, ^3Py, decreases with increasing solvent polarity [27,28].

4. Conclusions

Based on the steady-state and time-resolved fluorescence measurements in aqueous and ethanolic solutions, we have demonstrated that dynamic quenching of pyrene fluorescence by Ag^+ ions in polar solvents can lead to formation of an exciplex, $(^1Py\cdots Ag^+)^*$. In these systems, exciplex formation is accompanied by rapid equilibration with $^1Py^*$ and Ag^+ ions. Exciplex emission lifetimes in both solvents were much shorter than their corresponding monomer fluoresence lifetimes because the lowest excited exciplex singlet state has several competitive nonfluorescent pathways with large rate constants for relaxation to the ground state, such as the formation of the triplet state by intersystem crossing. The higher equilibrium constant for exciplex formation in aqueous solution indicates the stronger interaction that occurs between $^1Py^*$ and Ag^+ in water versus ethanol. Similarly, the higher exciplex quantum yield in aqueous solution indicates the enhanced stability of the exciplex in water versus ethanol, most likely because of the decreased efficiency of ISC in water versus ethanol.

Acknowledgements

We gratefully acknowledge the technical assistance of Mike McLeod and fruitful discussions with Dongqiang Zhu. We also appreciate the helpful review comments made by the two anonymous referees and by the editor, Professor Russell Schmehl. This manuscript is based upon work supported by the National Science Foundation under Grant No. 0096053.

References

[1] B. Stevens, Adv. Photochem. 8 (1971) 161.
[2] W.R. Ware, W. Watt, J.D. Holmes, J. Am. Chem. Soc. 96 (1974) 7853.
[3] K. Kalyanasundaram, Photochemistry in Microheterogeneous Systems, Academic Press, 1987.
[4] M.G. Kuzmin, Pure Appl. Chem. 65 (1993) 1653.
[5] I.R. Gould, R.H. Young, L.J. Mueller, S. Faria, J. Am. Chem. Soc. 116 (1994) 8176.
[6] I.R. Gould, R.H. Young, L.J. Mueller, A.C. Albrecht, S. Farid, J. Am. Chem. Soc. 116 (1994) 8188.
[7] M.C. Rath, H. Pal, T. Mukherjee, J. Phys. Chem. A 105 (2001) 7945.
[8] H. Dreeskamp, A. Laufer, Chem. Phys. Lett. 112 (1984) 479.
[9] A.G.E. Laufer, H. Dreeskamp, K.A. Zachariasse, Chem. Phys. Lett. 121 (1985) 523.
[10] M. Komfort, N. Rohne, H. Dreeskamp, M. Zander, Photochem. Photobiol. Chem. 71 (1993) 39.
[11] T. Saito, S. Yasoshima, H. Masuhara, N. Mataga, Chem. Phys. Lett. 59 (1978) 193.
[12] Y. Nosaka, A. Kira, M. Imamura, J. Phys. Chem. 85 (1981) 1353.
[13] T. Nakamura, A. Kira, M. Imamura, J. Phys. Chem. 86 (1982) 3359.
[14] J.H. Lee, M.A. Schlautman, E.R. Carraway, S. Yim, B.E. Herbert, J. Photochem. Photobiol., A. Chem. 163 (2004) 165.
[15] A.R. Watkins, J. Phys. Chem. 77 (1973) 1207.
[16] H. Masuhara, H. Shioyama, T. Saito, K. Hamada, S. Yasoshima, N. Mataga, J. Phys. Chem. 88 (1984) 5868.
[17] T.D. Gauthier, E.C. Shane, W.D. Guerin, W.R. Seitz, C.L. Grant, Environ. Sci. Technol. 20 (1986) 1162.
[18] J.R. Lakowicz, Principles of Fluorescence Spectroscopy; 2nd ed.; Kluwer Academy/Plenum Publisher, New York, 1999.
[19] K. Kalyanasundaram, J.K. Thomas, J. Am. Chem. Soc. 99 (1977) 2039.
[20] M.G. Kuzmin, L.N. Guseva, Chem. Phys. Lett. 3 (1969) 71.
[21] A. Weller, Z. Phys. Chem. N. F. 130 (1982) 129.
[22] N. Mataga, Pure Appl. Chem. 56 (1984) 1225.
[23] H. Pal, D.K. Palit, T. Mukherjee, J.P. Mittal, J. Photochem. Photobiol., A. Chem. 83 (1990) 391.
[24] N.J. Turro, Modern Molecular Photochemistry, University Science Books, Mill Valley, CA, 1991.
[25] F.P. Schwarz, S.P. Wasik, Anal. Chem. 48 (1976) 524.
[26] C.A. Parker, C.G. Hatchard, Trans. Faraday Soc. 59 (1963) 284.
[27] P. Van Haver, N. Helsen, S. Depaemelaere, M. Van der Auweraer, F.C. De Schryver, J. Am. Chem. Soc. 113 (1991) 6849.
[28] M. van der Auweraer, L. Viaene, P. Van Haver, F.C. De Schryver, J. Am. Chem. Soc. 97 (1993) 7178.